Mon. Not. R. Astron. Soc. **000**, 000–000 (0000) Printed 7 September 2018 (MN LaTeX style file v2.2)

HI Signal from Reionization Epoch

Shiv K. Sethi[1]
[1]*Raman Research Institute, Bangalore 560080, India*
emails: sethi@rri.res.in

7 September 2018

ABSTRACT

We investigate the all-sky signal in redshifted atomic hydrogen (HI) line from the reionization epoch. We model the phase of reionization as multiple point sources which carve out spherical Stromgren spheres. We study ionization histories compatible with WMAP observation. The Lyman-α and soft x-ray emission from these sources is taken into account for studying the HI signal. HI can be observed in both emission and absorption depending on the ratio of Lyman-α to ionizing flux and the spectrum of the radiation in soft xray. We also compute the signal from pre-reionization epoch and show that within the uncertainty in cosmological parameters, it is fairly robust. The main features of HI signal can be summarized as: (a) The pre-ionized HI can be seen in absorption for $\nu \simeq 10$–$40\,\mathrm{MHz}$; the maximum signal strength is $\simeq 70$–$100\,\mathrm{mK}$. (b) A sharp absorption feature of width $\lesssim 5\,\mathrm{MHz}$ might be observed in the frequency range $\simeq 50$–$100\,\mathrm{MHz}$, depending on the reionization history. The strength of the signal is proportional to the ratio of the Lyman-α and the hydrogen-ionizing flux and the spectral index of the radiation field in soft xray (c) At larger frequencies, HI is seen in emission with peak frequency between 60–$100\,\mathrm{MHz}$, depending on the ionization history of the universe; the peak strength of this signal is $\simeq 50\,\mathrm{mK}$. From Fisher matrix analysis, we compute the precision with which the parameters of the model can be estimated from a future experiment: (a) the pre-reionization signal can constrain a region in the $\Omega_b h^2$–$\Omega_m h^2$ plane (b) HI observed in emission can be used to give precise, $\lesssim 1\%$, measurement of the evolution of the ionization fraction in the universe, and (c) the transition region from absorption to emission can be used as a probe of the spectrum of ionizing sources; in particular, the HI signal in this regime can give reasonably precise measurement of the fraction of the universe heated by soft x-ray photons.

1 INTRODUCTION

One of the most important issues in modern cosmology is to understand the re-ionization of the universe. In the standard scenario the universe is mostly neutral for $z \lesssim 1000$ up to an epoch when the formation of first structures might have reionized the universe (e.g. Peebles 1993, Padmanabhan 2002, 1993). From Gunn-Peterson (GP) tests in past decades the intergalactic medium (IGM) was inferred to be almost fully ionized for $z \lesssim 5$ (see e.g. Barkana & Loeb 2001, Peebles 1993). Many recent observations suggest that universe might have been making a transition from fully ionized to neutral for $5.5 \lesssim z \lesssim 6.2$ (White et al. 2003, Fan et al. 2002, Djorgovski et al. 2001, Becker et al. 2001). Recent WMAP observations support a re-ionization epoch in the redshift range $z \simeq 10$–25 depending on the details of reionization (Kogut et al. 2003). Together GP and WMAP observations probably point to a complex reionization history in which the universe might have gone through two epochs of reionization (e.g. Mesinger & Haiman 2004, Wyithe & Loeb 2004b). Given these uncertainties it is therefore important that the phase of reionization is investigated using other probes. One such probe is based on observing the redshifted neutral hydrogen (HI) hyperfine line during reionization (see e.g. Scott & Rees 1990; Shaver et al. 1997).

The observable effect in this probe is the change in CMBR temperature at the redshifted frequency $1420/(1+z)\,\mathrm{MHz}$. Even in the pre-reionization era this change is non-zero and potentially detectable (Scott & Rees 1990). During reionization the signal is further complicated by Lyman-α and x-ray radiation fields (Madau, Meiksin, & Rees 1997). Madau et al. (1997) computed the expected HI signal around an ionizing source. More recently, Gnedin and Shaver (2004) studied the HI signal from hydrodynamic simulations. In this paper we attempt to model the phase of reionization semi-analytically to study the global HI signal. We model the phase of reionization as multiple ionizing sources, whose individual spherical Stromgren spheres expand to percolate, causing the universe to change from entirely neutral to a fully ionized phase (e.g. Haiman & Holder 2003). We compute the background HI signal in this semi-analytic model, taking into account the effect of different radiation fields. We also compute the signal from pre-ionization epoch and show that the present uncertainty in cosmological parameters are small enough to fix quite robustly the main features of this signal.

In addition to the background signal it is possible to consider fluctuations in the HI signal (e.g. Gnedin and Shaver 2004, Zaldarriaga, Furlanetto, & Hernquist 2004, Tozzi et al. 2000). Both single dish and interferometric experiments are being planned to detect the HI signal from the reionization epoch (Subrahmanyan 2004, `www.lofar.org`, Pen, Wu, & Peterson 2004). Future interferometric experiments like LOFAR have the potential to detect both the all-sky and the fluctuating component of the HI signal. In this paper we discuss only the all-sky signal. This signal is harder to detect owing largely to galactic and extragalactic foregrounds which have temperatures several orders of magnitude larger than the expected HI signal. However unlike the HI signal these foregrounds are expected to be featureless in frequency and therefore might be removable (see e.g. Zaldarriaga et al. 2004 and references therein).

In the next section we discuss the evolution of HI spin temperature in an expanding universe. In §3 we discuss the pre-ionization signal. In §4 we discuss in detail the semi-analytic model for the ionization history and the effects of Lyman-α and soft x-ray radiation fields in determining the HI signal. In §5 we present our main results. In §6 we discuss various uncertainties associated with our model and summarize our results. Throughout this paper, unless specified, we use the currently-favoured FRW model: spatially flat with $\Omega_m = 0.3$ and $\Omega_\Lambda = 0.7$ (Spergel et al. 2003, Perlmutter et al. 1999, Riess et al. 1998) with $\Omega_b h^2 = 0.02$ (Spergel et al. 2003, Tytler et al. 2000) and $h = 0.7$ (Freedman et al. 2001).

2 EVOLUTION OF HI SPIN TEMPERATURE

The HI spin temperature T_s is defined as:

$$\frac{n_2}{n_1} = 3\exp(-T_\star/T_s) \tag{1}$$

Here n_2 and n_1 are the populations of the hyperfine states. $T_\star = h\nu_\star/k = 0.06\,\mathrm{K}$; $\nu_\star = 1420\,\mathrm{MHz}$ is the frequency of hyperfine transition. In the early universe, the spin temperature is determined from detailed balancing between various processes that can alter the relative populations of the two levels (Field 1958, 1959):

$$T_s = \frac{T_{\rm CMBR} + y_c T_K + y_\alpha T_\alpha}{1 + y_c + y_\alpha} \tag{2}$$

Here $y_c = C_{21}/A_{21}T_\star/T_K$, $C_{21} \propto n_{\rm H}$ is the rate of collisional de-excitation of the upper level (Field 1958, Allison & Dalgarno 1969); $y_\alpha = D_{21}/A_{21}T_\star/T_\alpha$, $D_{21} \propto n_\alpha$ is the de-excitation rate of the upper triplet induced by Lyman-α photons, with n_α being the number density of Lyman-α photons (Field 1958). y_c and y_α correspond, respectively, to relative probabilities with which collisions between atoms and the presence of Lyman-α photons determine the level populations. T_K is the matter temperature and T_α is the 'temperature' of Lyman-α photons in the frequency range $\simeq \nu_\alpha \pm \nu_\star$ (Field 1959). Eq. (2) assumes that CMBR is the only radio source in the universe. In the epoch following the recombination and before the reionization starts this is evidently true; in our analysis we assume it to be the case even after the start of re-ionization. In the pre-reionization era, there are no Lyman-α photons, and therefore $y_\alpha = 0$. During reionization Lyman-α photons can play an important role in determining HI hyperfine level population. Eq. (2) is valid in the expanding universe so long as all the processes that determine the level population have rates far exceeding the expansion rate of the universe, and therefore the evolution of the spin temperature is determined by the slow expansion rate and is given by the values of different quantities at any given epoch; it can be shown that all the relevant rates are large enough for this approximation to hold (see e.g. Madau et al. 1997).

As CMBR is the only radio source at high redshifts, HI signal in hyperfine transition can be seen against the CMBR in emission or in absorption. The observed quantity then is the deviation of CMBR from a black body at frequency $\simeq \nu_\star$. The observed deviation at the present epoch is, at the observed frequency $\nu_0 = \nu_\star/(1+z)$:

$$\Delta T_{\rm CMBR} = -\frac{\tau_{\rm HI}}{(1+z)}(T_{\rm CMBR} - T_s) \tag{3}$$

Here $\tau_{\rm HI} = \sigma_\nu N_{\rm HI} T_\star/T_s$, with the HI column density $N_{\rm HI} = \int n_{\rm HI} d\ell$; $\sigma_\nu = c^2 A_{21}\phi_\nu/(8\pi\nu_\star)$; $A_{21} \simeq 1.8 \times 10^{-15}\,\mathrm{sec}^{-1}$ and ϕ_ν is the line response function. For a flat response function, $\phi_\nu = 1/\Delta\nu$, this can be expressed as (see e.g. Madau et al. 1997):

$$\tau_{\rm HI} = 0.02\left(\frac{\Omega_{\rm HI}h^2}{0.024}\right)\left(\frac{0.15}{\Omega_m h^2}\right)^{1/2}\left(\frac{T_{\rm CMBR}}{T_s}\right)\left(\frac{1+z}{20}\right)^{1/2} \tag{4}$$

Here $\Omega_{\rm HI}$ corresponds to the neutral fraction of hydrogen. Eqs. (3) and (4) can readily be extended to the case when the universe is a mixture of phases with different ionized fraction and spin temperature. We shall see later that it turns out to be the case when the universe makes a transition from a fully neutral to a fully ionized phase. It follows from Eq. (3) that the HI can be observed in either absorption or emission against CMBR depending on whether T_s is less than or exceeds $T_{\rm CMBR}$.

3 HI SIGNAL FROM PRE-REIONIZATION EPOCH

The pre-reionization signal has been computed previously by Scott and Rees (1990) and more recently by Loeb and Zaldarriga (2004). We re-compute and summarize this signal in this section. In particular we emphasize the robustness of this signal and its dependence of this signal on various cosmological parameters.

To calculate this signal we compute the evolution of matter temperature and ionized fraction of hydrogen in the post-recombination prior to the epoch of reionization (for relevant equations see e.g. Peebles 1993). To accurately determine the dependence of ionization fraction in the post-recombination universe on cosmological parameters, we begin integrating the equations at $z = 2000$. At this redshift the hydrogen is fully ionized, and the helium, 8% of the baryon number density, can be considered fully neutral.

At $z \simeq 1000$, $T_{\rm CMBR} = T_K$ and it follows from Eq. (2) that $\Delta T_{\rm CMBR} = 0$ (Scott & Rees 1990). For $z \lesssim 100$, $T_K < T_{\rm CMBR}$ and therefore HI can be observed in absorption against CMBR if $y_c \gtrsim 1$ (Eq. (3)). In Figure 1 we show the pre-ionization signal as a function of the observing frequency, $\nu_0 = \nu_\star/(1+z)$ for a universe that doesn't re-ionize for $z \gtrsim 10$. As discussed above, for $z \gg 100$, $T_s \simeq T_{\rm CMBR}$ and therefore the HI can be observed neither in emission nor in absorption. For $z \lesssim 100$, $y_c > 1$ and therefore $T_s \simeq T_K < T_{\rm CMBR}$; the HI can be observed in absorption against the CMBR. For $z \lesssim 20$, $y_c < 1$ and therefore $T_s \simeq T_{\rm CMBR}$ and $\Delta T_{\rm CMBR} \simeq 0$. Scott and Rees (1990) showed these main features of the absorption signal. However owing to uncertainties in the cosmological parameters like Ω_B and Ω_m neither the magnitude nor the frequency at which it will peak could be established. In recent year fairly precise determination of these cosmological parameters has become possible largely owing to CMBR anisotropy and large scale structure studies (e.g Spergel et al. 2003).

The main dependence of the absorption signal is on different cosmological parameters that determine the evolution of the matter temperature T_K and the probability of collisions y_c. In Figure 1 we also show the dependence of the HI signal on different cosmological parameters; the parameter range is taken to be 2σ around the central values and errors determined by WMAP (Spergel et al. 2003). It is seen from the figure that the location of the signal in frequency space and also its magnitude are fairly robust within the expected uncertainties in determining cosmological parameters. As we shall see below re-ionization at $z \simeq 15$ doesn't affect the main features of the absorption signal. This signal therefore is a unique probe of the thermal history of the universe. In a later section, we show how the detection of this signal can be used to determine cosmological parameters.

4 HI SIGNAL DURING RE-IONIZATION

In the standard ΛCDM model of structure formation in the universe, small inhomogeneities, which originated during an inflationary era in the very early universe, were amplified by gravitational instability. First structures in the universe formed when these perturbations became non-linear and collapsed (see e.g. Peebles 1993, Padmanabhan 2002, 1993 and references therein). The gravitational collapse of these structures might set off star-formation (alternatively some material might end up in black holes which by accreting more matter will radiate with harder spectrum than first star-forming galaxies, see e.g. Ricotti & Ostriker 2003) which will emit UV light and ionize the IGM. The process of re-ionization of the universe is generally quite complicated and not well understood (e.g. Barkana & Loeb 2001). However it is possible to study it within the framework of simple models which might give important clues about the details of this process. We assume that each collapsed object emits isotropically and causes a spherical ionization sphere around it. The reionization is completed when the fraction of volume occupied by these ionized spheres approaches unity. Important ingredients of this problem are: (a) Halo population at high redshift, (b) molecular and atomic cooling in Haloes, (c) Initial Mass Function of stars and star formation rate, (d) Escape fraction of UV photons from Haloes, (e) clumpiness of the IGM. Of these the most uncertain are (c) and (d) and have to be modelled using simple parameterized models. In addition to these uncertainties in modelling the ionization fraction of the universe, other considerations are needed to understand the HI signal during reionization. These complications can be appreciated by studying the signal around an isolated object. The ionizing radiation from the object will carve out a spherical ionizing front. The region outside this ionized sphere is mostly neutral and its HI signal can be observed. The object however emits not only the hydrogen-ionizing radiation but can emit radiation close to Lyman-α frequency and also in soft x-ray. These two radiation fields can penetrate beyond the ionized sphere and alter the level population of the HI. If the Lyman-α intensity is high enough the level population of HI is coupled to Lyman-α photons (Eq. (2)). In addition Lyman-α photons can slowly heat the HI gas by atom recoil (Madau et al. 1997). The soft x-ray photons can heat the gas beyond the ionized sphere by photo-electric absorption (Madau et al. 1997). As we shall study below, the region immediately beyond the ionized sphere is heated by soft x-ray photons to temperatures above $T_{\rm CMBR}$ and therefore will be seen in emission (Eq. 3). There are two possibilities for regions not heated by soft x-ray: (a) the spin temperature in these regions is $\simeq T_{\rm CMBR}$, and therefore these regions cannot be observed in either emission or absorption. (b) the spin temperature T_s in these regions is determined by the Lyman-α photons which means that $T_s \simeq T_\alpha \simeq T_K$. As $T_K \lesssim T_{\rm CMBR}$ in regions not yet heated by soft x-ray photons, the HI from these regions can be observed in absorption. As we shall see later, possibility (b) is realized in most situations.

4.1 Evolution of Ionized fraction

We take up various aspects of the evolution of the ionized component in this subsection.

The first important ingredient is the mass function of the collapsed dark matter haloes. In the ΛCDM models, the mass function at any redshift can be obtained from the Press-Schechter method (Press & Schechter 1974, for details see Pebbles 1993, Padmanabhan 2002, 1993). The number density of dark matter haloes per unit mass is:

$$\frac{dn}{dM} = \sqrt{\frac{2}{\pi}}\frac{\rho_m}{M}\delta_c(z)\left|\frac{d\sigma}{dM}\right|\frac{1}{\sigma^2(M)}\exp\left[-\delta_c(z)^2/(2\sigma^2(M))\right] \tag{5}$$

Here $\sigma(M)$ is the mass dispersion filtered at the scale corresponding to mass M in the linear theory; $\sigma(M)$ for length scale corresponding to $8h^{-1}\,\mathrm{Mpc}$ is $\simeq 0.9$ (Spergel et al. 2003); $\delta_c(z) \simeq 1.7D(0)/D(z)$, with $D(z)$ being the solution of growing mode in linear theory; in sCDM model $D(0)/D(z) = (1+z)$ (for details see Padmanabhan 2002, 1993, Peebles 1980). The collapsed fraction of all structures can be calculated from Eq. (5); for $z \simeq 20$ the collapsed fraction is $\simeq 2\times 10^{-3}$. Even though dark matter haloes of all masses will collapse and virialize, they will not be able to trap baryons unless the haloes have masses exceeding the Jeans mass of the IGM. The Jeans mass at $z \simeq 20$ is $\simeq 10^4\,\mathrm{M}_\odot$ (e.g. Barkana & Loeb 2001). Another important consideration is whether the baryons in the collapsed haloes can cool sufficiently rapidly to form stars (see e.g. Tegmark et al. 1997, Sethi 2004, Barkana & Loeb 2001); the smallest halo mass that satisfy this criterion is $M \simeq 10^7\,\mathrm{M}_\odot$. Our study shows that the evolution of ionization fraction (Eq. (7) is insensitive to the exact value of the mass of the smallest halo that can form stars. Another complication that is harder to incorporate in our analysis is that the Jeans mass in the regions which are ionized is very different from the regions which are neutral. In the ionized regions, $T_K \simeq 10^4\,\mathrm{K}$ and at $z \simeq 20$, this gives a Jeans mass $\simeq 10^9\mathrm{M}_\odot$. This is not an important consideration so long as the ionized fraction $f_{\rm ion} \ll 1$ (Eq. (7)). However once the ionized fraction approaches unity, the mass of the smallest haloe that can cool sufficiently to form stars should be comparable to the value of Jeans mass in the ionized region. We check how this affects the evolution of ionized fraction by retaining only haloes larger than the Jeans mass at that redshift in the ionized regions as the ionized fraction exceeds 0.5 and find that it makes an insignificant difference to the evolution of ionized fraction.

From information about the halo population and cooling arguments it is possible to speculate on the ionization history of the universe from photo-ionization. The main uncertainty is the hydrogen-ionizing luminosity (and its evolution) of each halo, which has to be parameterized. Assuming that halo of mass M emits isotropically the hydrogen-ionizing luminosity $\dot N_\gamma$ (in photons $\sec^{-1}$), the radius of ionizing sphere around the source will satisfy the equation (Stromgren Sphere, see e.g. Shu 1992, Shapiro & Giroux 1987, Wyithe & Loeb 2004b):

$$\frac{dR}{dt} - HR = \frac{(\dot N_\gamma - 4\pi/3R^3\alpha_B C n_b^2 x_{\rm HI})}{(\dot N_\gamma + 4\pi R^2 x_{\rm HI} n_b)} \tag{6}$$

Here $C \equiv \langle n_b^2\rangle/\langle n_b\rangle^2$ is the clumping factor of the IGM. In Eq. (6) the right hand side approaches unity as R tends to zero. This corresponds to the fact that initially Stromgren sphere expands at the speed of light (Wyithe & Loeb 2004b). At larger R, the $\dot N_\gamma$ term in the denominator can be dropped and the Stromgren sphere evolution equation approaches it usual form (e.g. Shapiro & Giroux 1987). Using Eq. (5), the fraction of the universe that is ionized at a given redshift is (see e.g. Haiman & Holder 2003):

$$f_{\rm ion}(z) = \frac{4\pi}{3}\int_0^z dz' \int dM \frac{dn}{dM}(M,z')R^3(M,z,z') \tag{7}$$

The minimum mass that can contribute to Eq. (7) is taken to be $10^7\,\mathrm{M}_\odot$. As discussed above the evolution ionized fraction is not very sensitive to the mass of smallest halo that can form stars. Further assuming that the luminosity of the source is $\propto M$, the ionized fraction can be calculated in terms of the evolution of the photon luminosity of a single halo of some fiducial mass and the evolution of the clumping factor. For simplicity we assume the clumping factor to have a constant value between one and five, and take the luminosity of the halo to be constant. Therefore, the photon luminosity of a halo of a given mass at any redshift can be expressed as:

$$\dot N_\gamma(M,t) = \left(\frac{M}{5\times 10^7\,\mathrm{M}_\odot}\right)\dot N_\gamma(0). \tag{8}$$

In Figure 2 we show several ionization histories for different values of $\dot N_\gamma(0)$ and clumping factor C. All the ionization histories shown in Figure 2 are consistent with WMAP observations which suggest that $\tau_{\rm reion} = 0.17 \pm 4$, 68% confidence level (Kogut et al. 2003) : the dot-dashed curve corresponds to $\tau_{\rm reion} = 0.22$ if the universe remains fully ionized after the first reionization; the dashed line gives, $\tau_{\rm reion} = 0.13$. It appears that $\dot N_\gamma \simeq 10^{50}$ is required to ionize the universe early enough to satisfy WMAP observations. This is just three orders of magnitude below the photon luminosity of a typical star-burst galaxy (see .e.g. Leitherer et al. 1999). Alternatively one can infer that the efficiency of the first star formation was very high (see e.g. Haiman & Holder 2003, Chiu, Fan & Ostriker 2003). There are other uncertainties like feedback from supernova, and photo-dissociation of molecular hydrogen which indicate this estimate is a lower limit (see e.g. Loeb & Barkana 2001, Haiman & Holder 2003, Haiman, Rees, & Loeb 1997, Dekel & Silk 1986). Alternatively it is possible that the collapsed fraction of the universe far exceeded the value given by ΛCDM models and was caused by some other physical process like tangled magnetic fields (Sethi & Subramanian 2005).

4.2 Evolution of HI signal

4.2.1 Effect of Lyman-α radiation

As discussed above the HI signal during re-ionization depends on the Lyman-α and x-ray flux from the objects. While the photons with frequencies around the ionization threshold are absorbed inside the Stromgren sphere, photons with frequencies between Lyman-α (1216 Å) and the ionization threshold (912 Å) in the rest frame of the object free-stream into the medium beyond the Stromgren sphere. (More exactly only photons between Lyman-α and Lyman-β frequencies can free-stream; higher frequency photons are absorbed locally by resonant transitions to higher levels (Lyman-β or above). This however makes no essential change to our inference here.) Assuming Lyman-α response function to be Dirac delta function, a photon of frequency ν between Lyman-α and the ionization threshold is absorbed by the resonant scattering at a comoving distance $\Delta R \simeq H_0^{-1}\Omega_m^{-1/2}(1+z)^{-3/2}\Delta\nu/\nu_\alpha$ with $\Delta\nu = \nu - \nu_\alpha$ in the expanding universe; $\Delta R \simeq 30h^{-1}\,\mathrm{Mpc}$ for $\nu \simeq 13.6\mathrm{eV}$. This defines the region of influence of the 'Lyman-α' photons around a source. Similar to ionized fraction, the fraction of the universe influenced by Lyman-α photons can be defined as:

$$f_\alpha(z) = \frac{4\pi}{3}\int_0^z dz' \int dM \frac{dn}{dM}(M,z') R_\alpha^3(z,z') \tag{9}$$

with $R_\alpha \simeq H_0^{-1}\Omega_m^{-1/2}(1+z)^{-5/2}\Delta z$ with $\Delta z = z' - z$. It can be readily seen that f_α rapidly reaches unity. In light of this fact, it is not necessary to study the region of influence around each source; instead it is possible to study the evolution of the mean intensity of the Lyman-α photons. The mean proper specific intensity of Lyman-α photons at high redshifts is given by:

$$I_{\nu_\alpha}(z) \simeq \frac{H_0^{-1}hc(1+z)^3}{4\pi\Omega_m^{1/2}} \int dM \int_z^{z_{\max}} dz' \frac{dn}{dM}\dot{N}_{\gamma\alpha}(M,z')(1+z')^{-5/2-\beta} \tag{10}$$

Here $\dot{N}_{\gamma\alpha}$ is the photon luminosity in Lyman-α photons of any object and β is the spectral index of the photons in the frequency range between Lyman-α and the Lyman continuum, ν_0. Here $1 + z_{\max} = (1+z)\nu_0/\nu_\alpha$ and is determined from the fact that photons above Hydrogen ionization threshold are absorbed locally. Given the uncertainty about the spectrum of the ionizing sources, we assume $\beta = 0$ and $\dot{N}_{\gamma\alpha} = A\dot{N}_\gamma$ i.e. the 'Lyman-α' luminosity (.i.e. the photon luminosity of the source in the wavelength range between Lyman-α and Lyman-β in the rest frame of the object) is a constant multiple of the luminosity of the Hydrogen-ionizing photons. From Eq. (2) it follows that the HI level population can be determined by the Lyman-α photons if $n_\alpha = 4\pi I_{\nu_\alpha}/(hc)$ is high enough to give $y_\alpha \gtrsim T_{\rm CMBR}/T_\alpha$. In the medium in which HI couples to Lyman-α, T_α tends to relax to T_K near the line center (Field 1959). Detailed calculations for an expanding universe show that this can occur in a time-scale shorter than the expansion time scale of the universe (Rybicki & Dell'antonio 1994). We will use $T_\alpha = T_K$ throughout this paper. In addition Lyman-α photons can also lead to heating of the HI from atom recoil (Field 1959, Madau et al. 1997). This heating rate however is generally quite small (Chen & Miralda-Escudé 2003) and we neglect it in our analysis. In Figure 3 and 4 we show the influence of Lyman-α radiation on the spin temperature. The figures show that for most models we consider the Lyman-α flux is large enough to couple spin temperature to the matter temperature for $z \gtrsim 20$. This result is in qualitative agreement with the analysis of Ciardi & Madau (2003).

4.2.2 X-ray Heating Outside Stromgren Sphere

To determine the the thermal evolution of HI during reionization we also need to take into account the heating of the HI from soft x-ray photons. If the ionizing sources emit soft x-ray photons, then these photons can reach beyond the Stromgren sphere and heat the surrounding HI from photo-electric absorption. The heating rate from the soft x-ray photons at a distance R from an ionizing source is:

$$\Delta\dot{E}_{\rm x} = f\frac{\dot{N}_\gamma h}{4\pi R^2}\int_{\nu_0}^\infty d\nu \nu^{-1-\alpha}\nu_0^\alpha \left[(\nu-\nu_0)\sigma_\nu^{\rm HI} + \chi(\nu-\nu_1)\sigma_\nu^{\rm HeI}\right]\exp(-\tau) \tag{11}$$

Here $\{\nu_0, \nu_1 = 13.6, 24.6\,\mathrm{eV}\}$ are the ionization threshold of Hydrogen and Neutral Helium, respectively; f, the fraction of soft x-ray photon energy deposited for heating the medium is a sensitive function of the ionized fraction, rising from nearly 0.1 for an ionized fraction $\simeq 2\times 10^{-4}$, the residual ionized fraction from recombination, to nearly one for the fully ionized medium (Shull & van Steenberg 1985). Soft x-ray photons will also partially ionize the medium (see below), thereby raising the ionized fraction above the value from recombination. The fraction of energy deposited in reionizing HI fall rapidly above the ionization fraction $\gtrsim 0.1$ (Shull & van Steenberg 1985). Therefore, without going into the details of the reionization from soft xray it is safe to assume that the ionization fraction remains $\lesssim 0.1$, as verified by the study of Venkatesan et al. (2001). For the class of model we study, we find that the ionization fraction due to reionization from soft x-ray photons varies from roughly 0.1 just outside the Stromgren sphere to 10^{-3} up to radii at which the x-ray heating can cause appreciable heating (for details see below). The fraction of heat deposited in this range of ionization fraction is $0.1 \lesssim f \lesssim 0.3$. As this is hard to self-consistently take into account at each radius, we use a constant, average, value $f = 0.2$ throughout this paper.

The heating due to ionization of singly ionized helium is negligible and is neglected here. $\chi = 0.08$ is the primordial Helium to Hydrogen ratio. We have assumed the spectrum of photons above hydrogen ionization threshold to fall as: $\nu^{-\alpha}$. $\sigma_\nu^{\rm HI}$ and $\sigma_\nu^{\rm HeI}$ are the cross-sections for Hydrogen and Helium ionization, respectively. $\tau = (n_{\rm HI}\sigma_\nu^{\rm HI} + n_{\rm HeI}\sigma_\nu^{\rm HeI})R$ is the optical depth to hydrogen and Helium ionization. In Eq. (11) we use the Newtonian expression for solving flux from a given source. This is justified as the size of the region influenced by the source $\ll H^{-1}(z)$. Eq. (11) is exact, however to solve it simplifications are needed. Firstly the ionization level of different species is required to self-consistently solve for the rate of energy injection. This however can be simplified by taking the gas to be fully ionized inside the Stromgren sphere and neutral outside the Stromgren sphere. This is justified as even though the soft x-ray photons will partially ionize the region outside the Stromgren sphere the ionization fraction is generally so small that the region can be considered totally neutral and therefore only the heating effect of these photons needs to be considered (for details see Venkatesan, Giroux & Shull 2001). Therefore we can take $R = r_s + r$, where r_s is the radius of Stromgren sphere and can be solved for each source separately. This simplification allows us to find the rate of energy injection from soft x-ray photons at a distance R from any source. As seen from Eq. (11), much of the contribution to this rate come from radii $R \lesssim 1/(n_{\rm HI}\sigma_\nu^{\rm HI})$; as $\sigma_\nu^{\rm HI}) \propto \nu^{-3}$ above the Hydrogen threshold, the region of influence of photons for different frequencies can be found. Eq. (11) is needed to address whether the matter temperature can be raised sufficiently above the CMBR temperature in this region of influence.

The evolution of matter temperature outside the Stromgren sphere can be found by including the energy injection from soft x-ray photons. However, from Eq. (3) we notice that once $T_s \gg T_{\rm CMBR}$ the HI emission is independent of the T_s or from Eq. (2) the matter temperature. Therefore for our study we do not need to solve for the detailed matter temperature profile outside a source, we only need to know the radius of the region in which $T_s \gg T_{\rm CMBR}$. This is ensured if $T_k \gg T_{\rm CMBR}$ and $y_\alpha \gtrsim 1$. The latter requirement is met in all the cases we consider. Therefore we calculate this radius by the following requirement: It is the radius in which the energy injection can raise the matter temperature $T_K = qT_{\rm CMBR}$, with $q \gtrsim 1$, in the local Hubble time, i.e. it is calculated from the expression:

$$\frac{\Delta \dot{E}_{\rm x}(R,z)}{H(z)k_B} = qT_{\rm CMBR} \qquad (12)$$

This allows us to define the fraction of volume which is influenced by x-ray, $f_{\rm x}$, similar to the ionization fraction. In Figure 5, we show the evolution of $f_{\rm x}$ for several values of the spectral index α and q. $q \simeq 1$ roughly determines the radius which demarcates the region seen in absorption from the region seen in emission. It should be pointed out that this prescription always gives an overestimate of the signal. This is because the HI signal in the transition region from absorption to emission is smaller than assuming a sharp boundary between the two regions. However this uncertainty is much smaller than the uncertainty in Lyman-α flux and the spectrum of the radiation field in soft xray, as seen in Figure 5. While presenting our results in the next section, unless specified otherwise, we use $q = 1$ throughout. In Figure 5, the dependence of $f_{\rm x}$ on the spectral index α is seen to be quite strong ; the observed signal, therefore, will hold the promise of unravelling the nature of ionizing sources.

In previous studies the the effect of x-ray heating in HI signal was taken into account by evolving the average specific intensity of the x-ray background (Chen & Miralda-Escude 2004). It would be possible to do it only if $f_{\rm x} \gg 1$. However, our study shows that, in contrast to Lyman-α photons, $f_{\rm x} \lesssim 1$ for a large range of redshifts of interest (Figure 5), i.e. the 'graininess' of the ionizing sources is important for x-ray heating. Even though both these approaches give similar results for the all-sky HI signal, the underlying physics is quantitatively quite different. In our study the HI signal doesn't make transition from absorption to emission by an increase in the average x-ray specific intensity but by coalescence of regions in which x-ray heating can raise the temperature of matter above CMBR temperature. In particular, the fluctuating component of the signal will be very different in the two cases. In the first case, the only scale in the problem is the size of the Stromgren sphere and the fluctuating component can be calculated by using methods such as developed by Zaldarriaga et al. (2004). In the latter case, the region affected by the x-ray around each source introduces a new scale in the problem and the fluctuating component is likely to be dominated by the gradients across the boundary of the transition region between absorption and emission. As future missions like LOFAR will have capability to observe in the redshift range where such effects might dominate, it is important to compute the fluctuating component of the HI signal for this multi-scale problem.

In this and the previous subsection, we have modelled the effect of Lyman-α and soft x-ray radiation in terms of two parameters: A and α. It could be asked what the different values of these parameter imply about the nature of sources of reionization. Given the uncertainty of star-formation history/quasar formation rate, the IMF, and metallicity of the sources at large redshifts, it is difficult to predict the spectrum of ionizing sources at those redshifts. This uncertainty motivates us to consider simple models parameterizable in terms of two parameters.

One possible way to speculate about the properties of these sources at high redshift is by analogy with low redshift sources. Observed quasars have a harder intrinsic spectrum $\alpha \simeq 1$ than is expected of star-forming galaxies for which $\alpha \lesssim 2.5$ (see e.g. Miralda-Escude & Ostriker 1990). Therefore by varying the value of α one could model sources of either kind. The value of A is very hard to estimate from observations at high redshifts. This is owing to the fact that much of flux short-ward of the Lyman-α is likely to be removed from scattering in the intervening IGM (see e.g. Barkana & Loeb 2001 and references therein). It should be pointed out that for this reason direct observation of ionizing sources by future telescopes like NGST also cannot reveal their nature. And the only possible way to estimate e.g. Lyman-α flux of these sources might be by its effect on the HI signal.

To summarize the discussion of the previous two subsections: main features of the HI signal during the reionization around a single ionizing source are: (a) In a region outside the Stromgren sphere, x-ray heating raises the temperature of the matter above CMBR temperature (Madau et al. 1997). If the Lyman-α radiation in this region is large enough, i.e. $y_\alpha \gtrsim 1$, to couple HI spin temperature to Lyman-α photons, then using $T_\alpha = T_K$, the HI in this region can be seen in emission. If the Lyman-α flux is not large enough, then HI continues to be coupled to CMBR and therefore cannot be observed in emission or absorption against CMBR. In all cases of interest $y_\alpha \gtrsim 1$ and therefore HI is seen in emission from this region. (b) photons between Lyman-α and Lyman-β frequencies penetrate deeper than the soft x-ray photons and therefore there are regions that are affected by Lyman-α photons but are not heated by x-ray. This leads to the possibility that while

HI gets coupled the Lyman-α photons, the matter temperature is still lower than CMBR temperature. In this case this region will be seen in absorption against the CMBR. We have extended this analysis to multiple sources distributed randomly throughout the universe which is valid so long as $f_{\rm ion} \lesssim 1$ or the individual Stromgren spheres do not intersect. (A stronger condition for the validity of such an analysis might be $f_{\rm x} \lesssim 1$; however it only means that once $f_{\rm x} \simeq 1$ all the HI in the universe can only be observed in emission.)

5 RESULTS

As discussed above and shown in Figure 1, the pre-ionization HI signal is fairly robust and only depends on the thermal history of the universe. The HI signal during re-ionization however is fairly complicated; Figures 2 to 5 capture this uncertainty in modelling the ionization and thermal history of the regions outside the ionizing region. Generically, the HI is seen in emission during reionization from the regions heated to temperature in excess of CMBR temperature from soft xray or it can be observed in absorption from region which are colder than CMBR but HI is coupled to Lyman-α radiation. The all-sky HI signal is a linear combination of these two components:

$$\Delta T_{\rm CMBR} = -\frac{\tau_{\rm HI}^{\rm em}}{(1+z)}(T_{\rm CMBR} - T_s^{\rm em}) - \frac{\tau_{\rm HI}^{\rm absor}}{(1+z)}(T_{\rm CMBR} - T_s^{\rm absor}) \tag{13}$$

As discussed in the previous section, the spin temperature in the region seen in absorption $T_s^{\rm absor} \simeq T_{\rm K}$ and the spin temperature in the region see in emission $T_s^{\rm em} \gg T_{\rm CMBR}$; $\tau_{\rm HI}^{\rm em} \propto (f_{\rm x} - f_{\rm ion})$ and $\tau_{\rm HI}^{\rm absor} \propto (1 - f_{\rm x})$; $\max\{f_{\rm x}, f_{\rm ion}\} = 1$. Using Eq. (4), Eq. (13) simplifies to:

$$\Delta T_{\rm CMBR} = 0.06\,{\rm K}\left[(f_{\rm x} - f_{\rm ion}) - (1 - f_{\rm x})\left(1 - \frac{T_s^{\rm absor}}{T_{\rm CMBR}}\right)\right]\left(\frac{\Omega_{\rm b}h^2}{0.024}\right)\left(\frac{0.15}{\Omega_m h^2}\right)^{1/2}\left(\frac{1+z}{20}\right)^{1/2} \tag{14}$$

In Figure 6, we show the HI signal for several ionization histories compatible with WMAP results; the dependence of the signal on the Lyman-α flux and the spectral index of radiation in soft xray is also shown. The main features of the HI signal are: (a) HI can be observed in absorption for $\nu \simeq 10$–$40\,{\rm MHz}$; the maximum signal strength is $\simeq 70$–$100\,{\rm mK}$. This is the signal from the pre-reionization epoch and as shown in Figure 1 is quite insensitive to the details of reionization. (b) A sharp absorption feature of width $\lesssim 5\,{\rm MHz}$ might be observed in the frequency range $\simeq 50$–$100\,{\rm MHz}$ depending on the reionization history. The strength of the signal is correlated with the ratio of the Lyman-α and the hydrogen-ionizing flux and the soft xray spectral index. (c) HI is seen in emission after the entire medium is heated to temperatures above $T_{\rm CMBR}$. This signal peaks between frequencies 60–$100\,{\rm MHz}$ depending on the ionization history of the universe and has peak strength $\lesssim 50\,{\rm mK}$. Our results are in qualitative agreement with the results of Gnedin & Shaver (2004). However the average signal we obtain is roughly a factor of two larger than obtained by Gnedin & Shaver (2004). We can partly understand it by comparing the ionization histories in our models with the fiducial ionization models studied by them (Figure 4 in Gnedin & Shaver (2004)). In the fiducial models they study, the ionization fraction has values $\gtrsim 0.5$ for $z \simeq 20$. In our ionization models, shown in Figure 2, the ionization fraction increases at a slower rate, and reaches values roughly $\lesssim 0.1$ by the epoch all the HI in the universe is heated above $T_{\rm CMBR}$ by the x-ray radiation.

5.1 Parameter estimation from HI signal

The HI signal shown in Figure 6 can be used to estimate parameters of the underlying models. We first list all the parameters used in our analysis: Cosmological parameters, Ω_m, Ω_b and h; parameters related to modelling ionization history: photon luminosity $\dot{N}_\gamma(0)$, clumping factor C; additional parameter needed for modelling HI signal: the ratio of Lyman-α to hydrogen-ionizing luminosity, A, and the spectral index of ionizing radiation in soft x-ray wave-band. This is the minimum set of parameters required to study the HI signal. It should be pointed out that using these parameters we attempt to model a physical process which might be inherently non-parameterizable. For instance we assume all the evolution of ionizing luminosity to be the same for all sources. However it is conceivable that all sources have different evolution and it is not possible in this analysis or even a more detailed simulation, to take that into account in a parametric form. However, we show in this section that it is possible to glean some generic properties of the HI signal in the parametric analysis.

HI signal can roughly be broken into three separate regimes: pre-reionization signal, transition from absorption to emission, HI observed in emission. We discuss each of these regimes in detail below and argue how these different regimes can be used to extract a sub-set of the parameters.

5.1.1 *Regime 1: The pre-reionization signal*

The all-sky HI signal in this regime doesn't depend on the details of reionization, i.e. in Eq. (14) $f_{\rm ion} = f_{\rm x} = 0$, but only on the cosmological parameters of the background universe. Before embarking on a detailed statistical analysis of this signal, we discuss the dependence of this signal on the cosmological parameters. Eq. (14) shows the dependence of this signal on $\Omega_b h^2$ and $\Omega_m h^2$. In addition, from Eq. (2), the spin temperature, T_s is seen to depend on $n_b \propto \Omega_b h^2$ and on the evolution of matter temperature. The evolution of matter temperature, T_K is determined by: (a) the local expansion rate. At large redshifts the expansion rate $H^2 \propto \Omega_m h^2$, independent of the dark energy content or the geometry of the universe and (b) the fraction of ionized hydrogen in the post-recombination universe, x_e; in the post-recombination universe prior to reionization $x_e \propto (\Omega_m^{0.5} h/\Omega_b h^2)$ (e.g. Peebles 1993). To summarize this discussion, the HI signal in the pre-reionization epoch depends on two parameters $\Omega_m h^2$ and $\Omega_b h^2$. Both these parameters can therefore be extracted from the observed HI signal. Future missions like LOFAR can potentially detect the HI signal for $\nu \gtrsim 20\,\mathrm{MHz}$ with RMS sensitivity $S_{\rm rms} \simeq 1\,\mathrm{mK}$ (the primary aim of LOFAR is to measure the fluctuating component of the signal; however the fluctuating component can be detected against a smoothly varying mean signal (Zaldarriaga et al. 2004), and therefore the mean is also potentially measurable). A similar sensitivity is being aimed for the single dish experiments which plan to detect only the all-sky signal (Subrahmanyan 2004). From Figure 6, the pre-reionization signal is seen to be the dominant signal for $\nu \lesssim 40\,\mathrm{MHz}$. We model the observed signal as six frequency bins separated by $4\,\mathrm{MHz}$ between $20\,\mathrm{MHz}$ and $40\,\mathrm{MHz}$ with signal determined to an RMS accuracy $S_{\rm rms}$ in each bin (the signal as seen from Eq. (14) doesn't depend on the bin width). We perform Fisher matrix analysis for the HI signal given by the central values of parameters $\Omega_m h^2 = 0.14$ and $\Omega_b h^2 = 0.024$, as determined by WMAP, to extract information about these parameters. The Fisher matrix can be written as (for a detailed discussion on Fisher matrix see e.g. Tegmark, Taylor & Heavens 1997):

$$\mathcal{F}_{ij} = \sum_k \frac{\partial(\Delta T_{\rm CMBR}(\nu_k))}{\partial\theta_i}\frac{1}{S_{\rm rms}^2}\frac{\partial(\Delta T_{\rm CMBR}(\nu_k))}{\partial\theta_j} \tag{15}$$

Here $\theta_i = \{\Omega_b h^2, \Omega_m h^2\}$ are the parameters to be determined and k signifies summing over the frequency bins.

In Figure 7 we show the 2-σ contours for the parameters for two assumed values of $S_{\rm rms}$. As seen from the figure, none of the two parameters are well determined but a line of degeneracy is picked (we confirm this from principal component analysis of the Fisher matrix (see .e.g. Bond & Efstathiou 1999)), which suggests that what is well determined is some weighted ratio of the two parameters. This is owing to the fact that the parameter dependence is dominated by the pre-factor of Eq. (14) which gives such a ratio.

How does the determination of parameters $\Omega_b h^2$ and $\Omega_m h^2$ compare with other measurements? $\Omega_b h^2$ can be determined to a reasonably precision from nucleosynthesis arguments (e.g. Tytler et al. 2000) and is the best determined parameter from the CMBR anisotropy measurements (Spergel et al. 2003, Efstathiou & Bond 1999); recent WMAP results give: $\Omega_b h^2 = 0.024 \pm 0.001$ (1σ). $\Omega_m h^2 \simeq 0.14 \pm 0.02$ (1σ) from recent WMAP observation and is determined largely by the early integrated Sachs-Wolfe effect (e.g Efstathiou & Bond 1999). Also, the galaxy power spectrum depends on $\Omega_m h^2$ with a weak dependence on Ω_b (e.g. Bond 1996, Peebles 1993). Therefore, the analysis of the observed galaxy power spectrum at $z \lesssim 0.5$ gives independent information on this parameter which can be used in conjunction with WMAP data to give tighter bounds on parameters (e.g Tegmark et al. 2004). Figure 7 shows that it not possible to give meaningful bounds on both $\Omega_m h^2$ and $\Omega_b h^2$. However, if we use prior information on one of the parameters then the other parameter can be determined with reasonable precision. For instance if we use the prior, given by 1σ error on the parameter, provided by WMAP data on the value of $\Omega_b h^2$, then we obtain $\Omega_m h^2 \simeq 0.15 \pm 0.03$ (1σ) for $S_{\rm rms} = 1\,\mathrm{mk}$, which is comparable to the precision of independent measurement of this parameter from WMAP. Therefore the pre-reionization HI signal could give important complementary information on cosmological parameters. It should be pointed out that the information on $\Omega_m h^2$, unlike the information from CMBR anisotropies and galaxy surveys, is completely independent of the geometry or the dark energy content of the universe, as it comes from the local expansion rate which is not affected by the geometry of the universe or the dark energy at $z \simeq 35$.

5.1.2 *Regime 2: HI seen in emission*

As seen in Figure 6, this part of the signal, assumed to last from the maximum of the signal to the frequency at which the universe is fully ionized, can vary substantially depending on the ionization history of the universe. For the two ionization histories shown in Figure 6, the signal is observable from $\simeq 60\,\mathrm{MHz}$ to $\simeq 100\,\mathrm{MHz}$ or from $\simeq 80\,\mathrm{MHz}$ to $\simeq 120\,\mathrm{MHz}$. In this regime also, the signal assumes reasonably simple form as $f_{\rm x} \gtrsim 1$, or all the HI in the universe is observable in emission; also in this regime, the signal doesn't depend on the Lyman-α flux as $T_s \simeq T_K \gg T_{\rm CMBR}$, and therefore the HI signal is nearly independent of T_s. The main dependence of the HI signal in this regime is on the cosmological parameters earlier discussed and the ionized fraction of the universe. The ionized fraction is determined by photon luminosity $\dot{N}_\gamma(0)$, the clumping factor C and $\Omega_m h^2$ and $\Omega_b h^2$, through the matter power spectrum used to determine the abundance of haloes (e.g Bond 1996).

First we consider the evolution of a single Stromgren sphere. During this evolution, the second term on the right hand side of Eq. (6) is generally sub-dominant (Shapiro & Giroux 1987), and therefore the dependence of the ionized fraction on the clumping factor and the baryon density is generally weak, though not negligible if the clumping factor is large, as see from Figure 3. In most cases, the evolution of a single Stromgren sphere is largely determined by the ratio: $\dot{N}_\gamma(0)/(\Omega_m h^2)$.

The other dependence of the HI signal on $\Omega_m h^2$ comes from the matter power spectrum that determines the abundance of dark matter haloes (e.g. Bond 1996, Eq. (5)). In addition, the pre-factor of Eq. (14) give the dependence on $\Omega_b h^2$ and $\Omega_m h^2$.

For Fisher matrix analysis we consider the following three parameters: the photon luminosity, $\dot{N}_\gamma(0)$, $\Omega_m h^2$, and $\Omega_b h^2$. For this analysis we take the HI signal to correspond to: $\dot{N}_\gamma(0) = 10^{49}\,\mathrm{sec}^{-1}$, $C = 1$ and $\Omega_b h^2 = 0.024$and $\Omega_m h^2 = 0.14$, the central values of determined by WMAP. Further, we assume $S\mathrm{rms} = 1\,\mathrm{mK}$ and 10 bins separated by $4\,\mathrm{MHz}$ in the frequency range $84\,\mathrm{MHz}$ to $120\,\mathrm{MHz}$.

The principal component analysis of the Fisher matrix yields the following ratios of the eigenvalues: $\lambda_1 : \lambda_2 : \lambda_3 = \{1, 0.02, 3\times10^{-8}\}$, with the eigenvectors, in the order of decreasing eigenvalues, dominated by $\Omega_b h^2$, $\Omega_m h^2$ and $\dot{N}_\gamma(0)$. The 1σ errors on parameters are: $\Delta\Omega_b h^2/\Omega_b h^2 = 0.04$, $\Delta\Omega_m h^2/\Omega_m h^2 = 0.07$ and $\Delta\dot{N}_\gamma(0)/\dot{N}_\gamma(0) = 0.8$. Therefore even though the cosmological parameters are well determined, the photon luminosity is poorly determined. This can be understood in terms of the evolution of a single Stromgren sphere. The dynamics of a single Stromgen sphere (Eq. (6)) is determined by the ratio $\dot{N}_\gamma(0)/(\Omega_m h^2)$ which causes this degeneracy. It should be noted that this degeneracy is generic to any model which envisages the reionization of the universe in terms of expanding Stromgen spheres. However, it is possible to break the degeneracy by using prior information on the cosmological parameters, as, as discussed above, the cosmological parameters can be determined to high precision by other measurements like CMBR anisotropy. Using the prior on the cosmological parameters as 1σ error bars from WMAP measurement, the error on $\dot{N}_\gamma(0)$ is nearly halved. In Figure 8 we show the contour levels in $\dot{N}_\gamma(0)$–$(\Omega_m h^2)$ plane for $\Omega_b h^2$ fixed to the central value of WMAP. From Figure 8 it is seen that the photon luminosity, $\dot{N}_\gamma(0)$ can be determined to an accuracy of around 50%. Future CMBR experiment Planck will measure the cosmological parameters to a much higher precision (e.g. Efstathiou & Bond 1999). Using the expected 1σ error bars for Planck measurements as priors, assumed here for simplicity to be a factor of 5 smaller than the WMAP errors, the photon luminosity, $\dot{N}_\gamma(0)$ can be determined to better than 20% relative precision.

In the foregoing we attempt to determine the evolution of ionization fraction in terms of the physical parameters like photon luminosity. In this case the ionized fraction in all bins is correlated as it is determined by the same underlying physical parameters. Instead one could try to directly determine the ionization fraction in each observable bin, independent of the underlying physical model.

In Fisher matrix analysis the ionization fraction in each bin can be treated as an independent parameter to be determined .i.e. $\theta_i = \{f_{\rm ion}(\nu_i)\}$, here ν_i gives the central frequencies of the bins. In our analysis we therefore consider 12 parameters: $\{\theta_1, \theta_2\} = \{\Omega b h^2, \Omega_m h^2\}$ and $\theta_i(i = 3, \cdots 12) = \{f_{\rm ion}(\nu_i)\}$. Owing to the linearly of the HI signal on the ionized fraction, the derivative of the signal with respect to parameters corresponding to the ionized fraction in each bin is rendered diagonal:

$$\frac{\partial(\Delta T_{\rm CMBR}(\nu_k))}{\partial\theta_i} \propto \delta_{ik} \tag{16}$$

Here δ_{ij} is the Kronecker delta function, and i is in the range between 3 and 12. The Fisher matrix reduces to:

$$\mathcal{F}_{ij} = \sum_k \frac{\partial(\Delta T_{\rm CMBR}(\nu_k))}{\partial\theta_i}\frac{1}{S^2_{\rm rms}}\frac{\partial(\Delta T_{\rm CMBR}(\nu_k))}{\partial\theta_j} P_{ij} \tag{17}$$

Here $P_{ij} = \delta_{ij}$ for i and j both between from 3 to 12, and $P_{ij} = 1$ otherwise. Using the priors on cosmological parameters from WMAP, $S_{\rm rms} = 1\,{\rm mk}$ and the model for HI signal as in the previous case, the relative precision on each parameter is: $\Delta\theta_i/\theta_i \lesssim 0.01$ .i.e. the ionized fraction can be estimated be a precision of nearly 1%. It should be pointed out that for the model of HI signal we use the ionization fraction increases from 0.15 to 1 in the frequency range we consider. These errors are comparable to the errors one would obtain by fixing the values of cosmological parameters to the central value given by WMAP; in which case the Fisher matrix is diagonal. And the errors on the ionization fraction is simply the square-root of the inverse of the diagonal elements. We also did the same analysis for different choices of parameters and arrive at similar results.

To summarize this discussion: we discuss two possible way of extracting the ionization history of the universe from the observed HI signal. In one case one could attempt to estimate the underlying physical parameters like the photon luminosity of the halo of some fiducial mass. On the other hand, it is conceivable that the ionization history is very complicated (e.g. Gnedin & Shaver (2004) discuss many complicated reionization histories) and it may not be possible to readily extract the underlying physical parameters. In that case one could try to directly estimate the ionization fraction in each observable bin. We show that it is possible to estimate the ionization fraction to a relative precision $\simeq 1\%$ (for ionization fraction exceeding roughly 0.15 in each bin) from future experiments. This is comparable to the determination of the ionization history from future CMBR experiments (Kaplinghat et al. 2003).

5.1.3 Regime 3: Transition from absorption to emission

The HI signal in this regime carries information about the spectrum of the ionizing sources. We have modelled the spectrum of sources by two parameters: the ratio of Lyman-α to hydrogen-ionizing luminosity, A and the spectrum of ionizing radiation in soft-xray radiation, α. The main observable features in this regime, as seen in Figure 6, are a possible narrow trough in the frequency range $50\,{\rm MHz}$ to $80\,{\rm MHz}$ and the rise to the maximum of the HI signal in emission. As seen in Figure 6, the amplitude of the HI trough is quite sensitive to the two parameters we use to model the spectrum of ionizing sources. The ionization fraction in this regime is $f_{\rm ion} \lesssim 0.1$ and therefore not very important to understand the main features of the signal.

As in the previous two cases, we can perform a Fisher matrix analysis for an assumed HI signal. The choice of parameters to get maximum information, as discussed in the previous case, is important. It is possible to extract information about A and α or alternatively, as in the previous discussion, one could directly attempt to measure $f_{\rm x}$ in each bin. We adopt the latter approach as it would also be applicable to a more complicated signal.

For our analysis, we take the underlying ionization model to be the same as in the previous case with $A = 20$ and $\alpha = 1.5$. To take into account the narrowness of the features in this regime we consider 25 bin, each $1\,{\rm MHz}$ wide in the frequency range $55\,{\rm MHz}$ to $80\,{\rm MHz}$. We consider 26 parameters: A and the values of $f_{\rm x}$ in each observable bin: $\theta_i(i = 2, \cdots 26) = \{f_{\rm x}(\nu_i)\}$; the cosmological parameters are assumed to be fixed to the central values determined by WMAP. As discussed above, the Fisher matrix in this case takes a simple form as the signal is linear in $f_{\rm x}$ which give 25 of the 26 assumed parameters (Eq. 17). For $S_{\rm rms} = 1\,{\rm mK}$, all the principal components of the Fisher matrix are well estimated (except the one corresponding to the frequency at which the HI signal vanishes). From these components we show that: $\Delta A/A \simeq 0.1$. The percentage errors on the $f_{\rm x}$ are shown in Figure 9. The error on A is quite sensitive to the assumed value of A and α. For instance for $A \lesssim 2$ and $\alpha \lesssim 3$, no meaningful bound can be obtained on A. In other words, the value of A cannot be determined unless a trough in HI signal is observed. The determination of $f_{\rm x}$ in each bin for $f_{\rm x} \gtrsim 0.25$, however, is less sensitive to the underlying model. We test this with models with different cosmological parameters and A and find that the fractional errors shown in Figure 9 are fairly indicative in these cases also.

In this subsection, we have shown how the observed HI signal can be used to get information about cosmological parameters and the ionizing sources. Our analysis allows us to glean the important information about the underlying parameters in each of the three regimes we consider. We attempt to estimate parameters we use in the modelling of the HI signal, like cosmological parameters, $\dot{N}_\gamma(0)$ and A. We also discuss methods which could give generic information like the ionization fraction or the fraction of universe heated by soft x-ray photons in an observable frequency bin. These methods would also be applicable to a more complicated HI signal.

6 DISCUSSION

In the foregoing sections, we discussed the ramifications of various simplifying assumptions we make. In this section we discuss many other effects of the our assumptions. In our analysis we do not take into effect the clustering of ionizing sources. The first objects to collapse in $\Lambda\mathrm{CDM}$ model are typically 3.5σ peaks of the density field (e.g. Barkana & Loeb 2001), and consequently their centers would have been more clustered than the density field by a factor of $\simeq 10$ (Kaiser 1984, for details see Peebles 1993, Padmanabhan 1993 and references therein). This is important for studying the fluctuating component of the HI signal (e.g. Wyithe & Loeb 20004a). However, this makes insignificant difference to $f_{\rm ion}$ because the volume of the Stromgren sphere scales roughly with the luminosity of the source (e.g. Madau et al. 1997). The effect of clustering on $f_{\rm x}$ is harder to access. While the energy injection (Eq. (11)) is proportional to the luminosity of the source, the radius, determined from Eq. (12), doesn't lend itself to some obvious scaling with the source luminosity. However, it is possible to draw some general conclusions. The radius is largely determined by the exponent in Eq. (11) which is independent of the source luminosity. The effect of clustering would be a smaller number of 'ionizing centers' with higher luminosities, and therefore $f_{\rm x}$ is expected to be smaller in this case. This uncertainty in $f_{\rm x}$, though important, is likely to be within the uncertainty from the spectrum of radiation in the soft xray (Figure 6). Therefore the suite of models we present in Figure 7 give a realistic picture of the evolution of the HI signal.

It is possible to consider more complicated models of the ionizing sources (e.g. Haiman & Holder 2003, Sethi 2004). It is conceivable that each ionizing source underwent one episode of star-burst activity and most of the ionizing photons were emitted during this epoch. Such models do not give qualitatively new ionizing histories (e.g. Sethi 2004); and the main features of the HI signal are unlikely to be affected by it. Here we only attempt to model the first phase of reionization, as required by the WMAP observation. Recent GP observations suggest the universe might have gone through two phases of reionization (Mesinger & Haiman 2004, Wyithe & Loeb 2004b). While this might change the HI signal for $z \simeq 6$, it is unlikely to affect the main features of the HI signal from higher redshifts we consider here.

Shaver et al. (1998) considered the detectability of the all-sky HI signal and concluded that signal-to-noise is not an important issue in this measurement. At observed frequencies $\simeq 50\,\mathrm{MHz}$, the system temperature is expected to be $\gtrsim 1000\,\mathrm{K}$, for a bandwidth of $\simeq 1\,\mathrm{MHz}$, a 5-σ detection is possible in an integration time of several hours. The main difficulties are system calibration and galactic and extra-galactic foregrounds. Galactic and extra-galactic foreground are expected to be smooth in frequency space and therefore potentially removable (Shaver et al. 1998, Zaldarriaga et al. 2004, Gnedin & Shaver 2004 and references therein). Calibration issues are being addressed in on-going searches for the all-sky signal (Subrahmanyan 2004).

ACKNOWLEDGMENT

We would like to thank Jayaram Chengalur, K. S. Dwarakanath, Zoltan Haiman, Biman Nath, Anish Roshi, Kandaswamy Subramanian, and Ravi Subrahmanyan for for many useful discussions. We also thank Zoltan Haiman, Ravi Subrahmanyan, and Biman Nath for detailed comments on the manuscript.

REFERENCES

Allison, A. C. and Dalgarno, A., 1969, ApJ, 158, 423
Barkana, R. and Loeb, A. 2001, Phys. Rep., 349, 125
Becker, R. H. et al. 2001, AJ, 122, 2850
Bond, R., in Schaeffer, R., Silk, J., Spiro, M., & Zinn-Justin, J. 1996, ASP
Chen, X. and Miralda-Escudé, J. 2004, ApJ, 602, 1
Chiu, W. A., Fan, X. & Ostriker, J. P 2003, ApJ, 599, 759
Ciardi, B. & Madau, P. 2003, ApJ, 596, 1
Dekel, A. & Silk, J. 1986, ApJ, 303,
Djorgovski, S. G., Castro, S., Stern, D., & Mahabal, A. A. 2001, ApJL, 560, L5
Efstathiou, G. & Bond, J. R. 1999, MNRAS, 304, 75
Fan, X., Narayanan, V. K., Strauss, M. A., White, R. L., Becker, R. H., Pentericci, L., & Rix, H. 2002, AJ, 123, 1247
Field, G. 1959, ApJ, 129, 551
Field, G. 1958, Proc. IRE, 46, 240

Freedman, W. L. et al. 2001, ApJ, 553, 47
Gnedin, N. & Shaver, P. 2004, ApJ, 608, 611
Haiman, Z. & Holder, G. 2003, ApJ, 595, 1
Haiman, Z., Rees, M. & Loeb, A. 1997, ApJ, 476, 458
Kaiser, N. 1984, ApJL, 284, 9
Kaplinghat, M., Chu, M., Haiman, Z., Holder, G. P., Knox, L. & Skordis, C. 2003, ApJ, 583, 24
Kogut, A. et al, 2003, ApJS, 148, 161
Leitherer et al 1999, ApJS, 123, 3
Madau, P., Meiksin, A., & Rees, M. J. 1997, 475, 429
Mesinger, A. and Haiman, Z. 2004, ApJL, 611, 69
Miralda-Escude, J., & Ostriker, J. P. 1990, ApJ, 350, 1
Padmanabhan, T. 2002, Theoretical Astrophysics, Volume III: Galaxies and Cosmology, Cambridge, UK: Cambridge University Press
Padmanabhan, T. 1993, Structure formation in the universe, Cambridge, UK: Cambridge University Press
Peebles, P. J. E. 1993, Principles of Physical Cosmology, Princeton University Press
Peebles, P. J. E. 1980, The Large Scale Structure of the Universe, Princeton University Press
Pen, U.-L., Wu, X.-P., Peterson, J. 2004, astro-ph/0404083
Perlmutter, S. et al. 1999, ApJ, 517, 565
Press, W. H. and Schechter, P. 1974, ApJ, 187, 425
Ricotti, M. & Ostriker, J. P. 2004, MNRAS, 352, 547
Riess, A. G. et al. 1998, AJ, 116, 1009
Rybicki, G. B. & Dell'Antonio, I. P. 1994, ApJ, 427, 603
Scott, D. and Rees, M. J. 1990, MNRAS, 247, 510
Shapiro, P. & Giroux, M. L. 1987, ApJ, 321, L107
Sethi, S. K. 2004, astro-ph/0411050, to appear in current science
Sethi, S. K. & Subramanian, K. 2005, MNRAS, 356, 778
Shaver, P. A., Windhorst, R. A., Madau, P. & de Bruyn, A. G. 1999, A&A, 345, 380
Shu, F. H. 1992, Physics of Astrophysics, Vol II: Gas Dynamics, University Science Books
Shull, J. M. & van Steenberg, M. E. 1985, ApJ, 298, 268
Spergel, D. N. et al. 2003, ApJS, 148, 175
Subrahmanyan, R. 2004, Cosmological Reionization Experiment, ATNF (private communication)
Tozzi, P., Madau, P., Meiksin, A. & Rees, M. J. 2000, ApJ, 528, 597
Tegmark, M., Taylor, A. N. & Heavens, A. F. 1997, ApJ, 480, 22
Tegmark, M. et al. 2004, Phys. Rev. D., 69, 103501
Tegmark, M., Silk, J., Rees, M. J., Blanchard, A., Abel, T., & Palla, F 1997, ApJ, 474, 1
Tytler, D., O'Meara, J. M., Suzuki, N., & Lubin, D. 2000, Physics Reports, 333, 409
Venkatesan, A., Giroux, M. L. & Shull, J. M. 2001, ApJ, 563, 1
White, R. L., Becker, R. H., Fan, X. & Strauss, M. A. 2003, ApJ, 126, 1
Wyithe, J. S. B. & Loeb, A. 2004a, Nature, 432, 194
Wyithe, J. S. B. & Loeb, A. 2004b, Nature, 427, 815
Zaldarriaga, M., Furlanetto, S. R. & Hernquist, L. 2004, ApJ, 608, 622

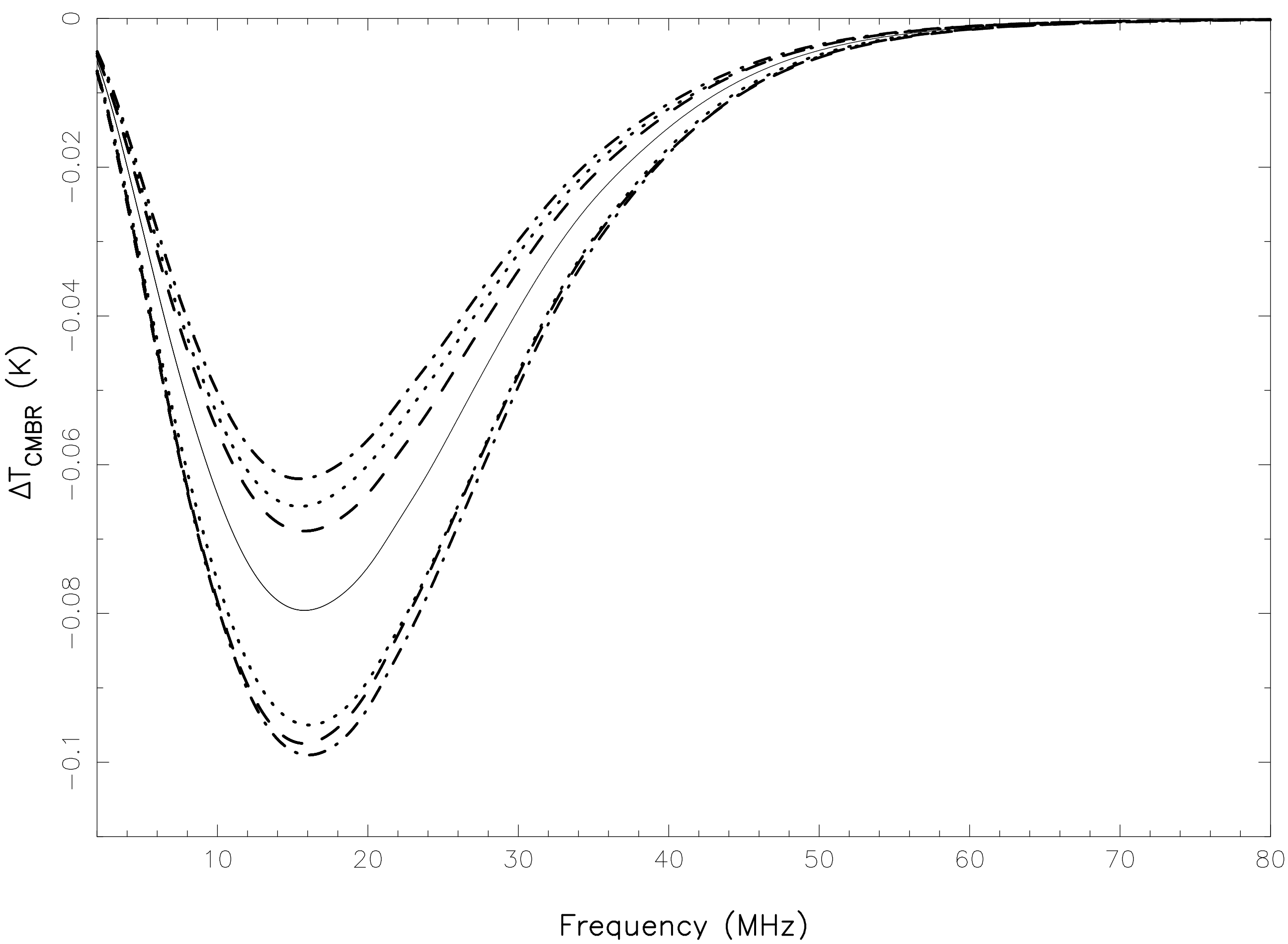

Figure 1. The pre-ionization HI signal is shown as a function of observing frequency. The solid line corresponds to the best fit parameters from WMAP: $\Omega_m = 0.3$, $\Omega_b = 0.047$, $h = 0.72$. Dotted, dashed, and dot-dashed lines give the 2-σ envelope from WMAP observations for Ω_m, Ω_b and h, respectively, around the best-fit model

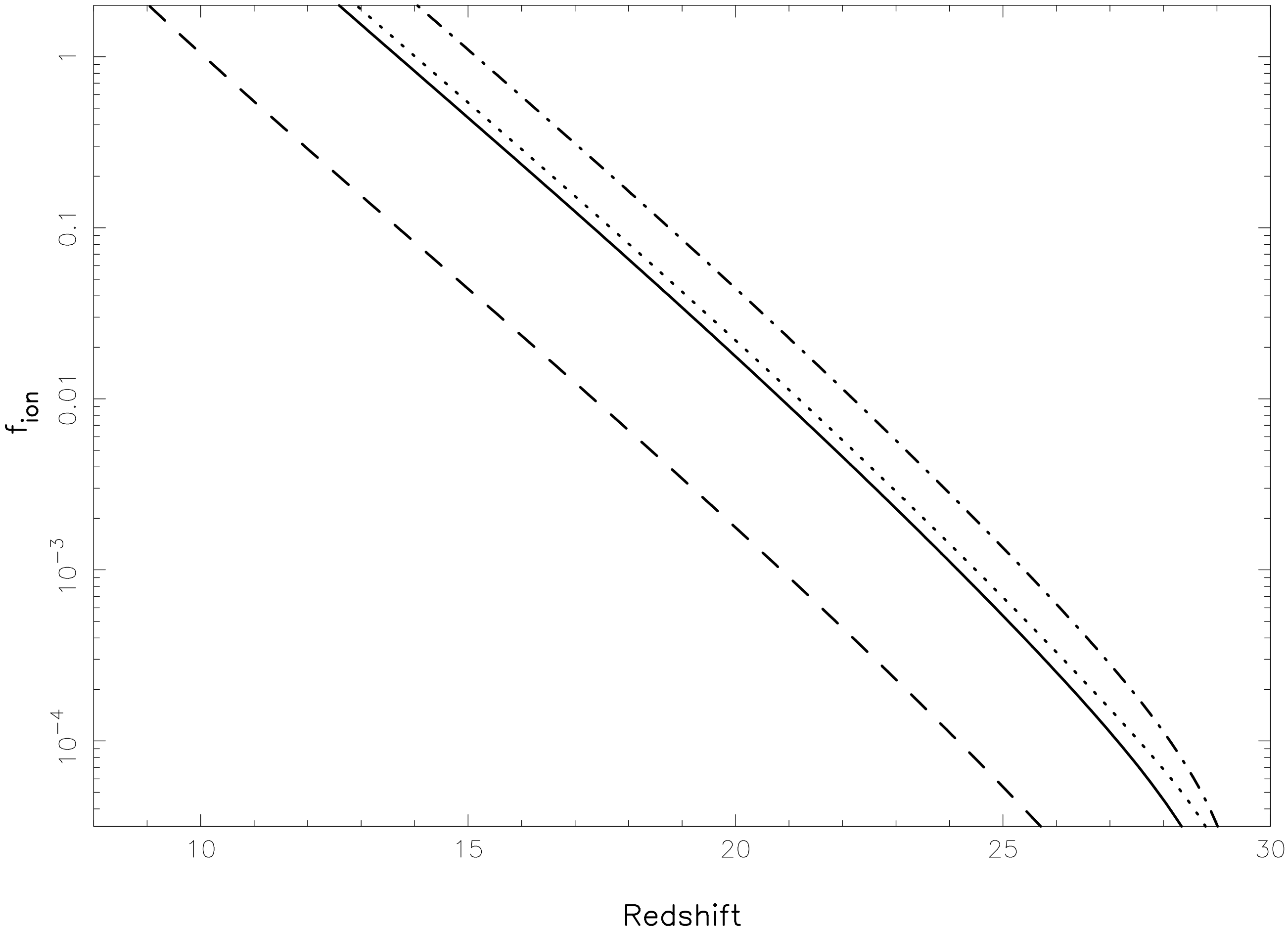

Figure 2. The evolution of ionized fraction is shown for several models: $\dot{N}_\gamma(0) = 10^{50}\,\mathrm{sec}^{-1}$, $C = 1$ (Solid line), $\dot{N}_\gamma(0) = 3 \times 10^{50}\,\mathrm{sec}^{-1}$, $C = 1$ (dot-dashed line), $\dot{N}_\gamma(0) = 10^{49}\,\mathrm{sec}^{-1}$, $C = 1$ (dashed line),$\dot{N}_\gamma(0) = 3 \times 10^{50}\,\mathrm{sec}^{-1}$, $C = 4$ (dotted line)

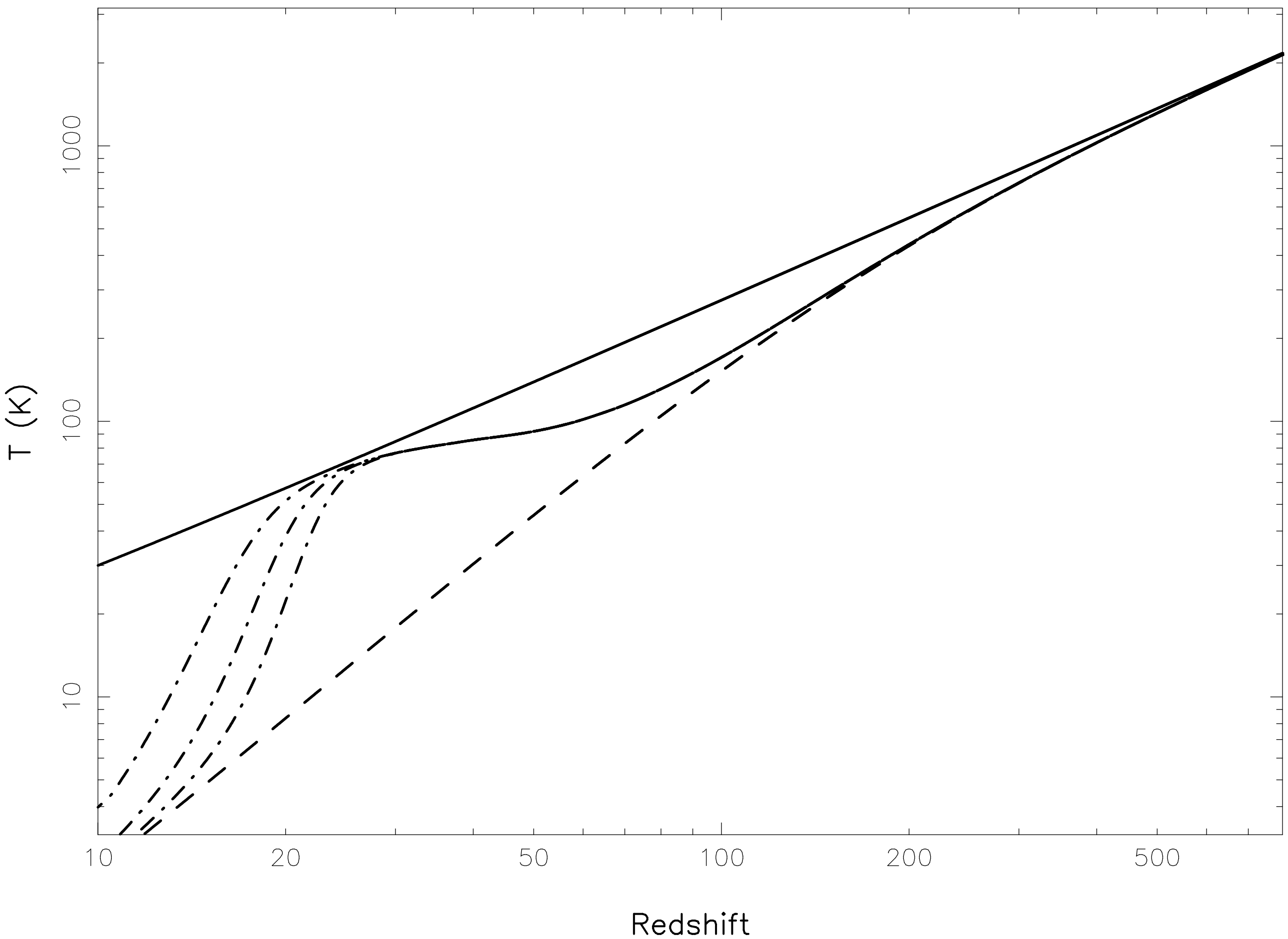

Figure 3. The evolution of spin temperature is shown for regions of the universe affected by Lyman-α radiation but not yet heated by the x-ray. The three dot-dashed lines correspond, from bottom to top, to a re-ionization model with $\dot{N}_\gamma(0) = 10^{50}\,\mathrm{sec}^{-1}$, and the ratio of Lyman-α to ionizing flux $A = \{40, 10, 2\}$, respectively. The solid and dashed lines correspond to CMBR and matter temperature, respectively.

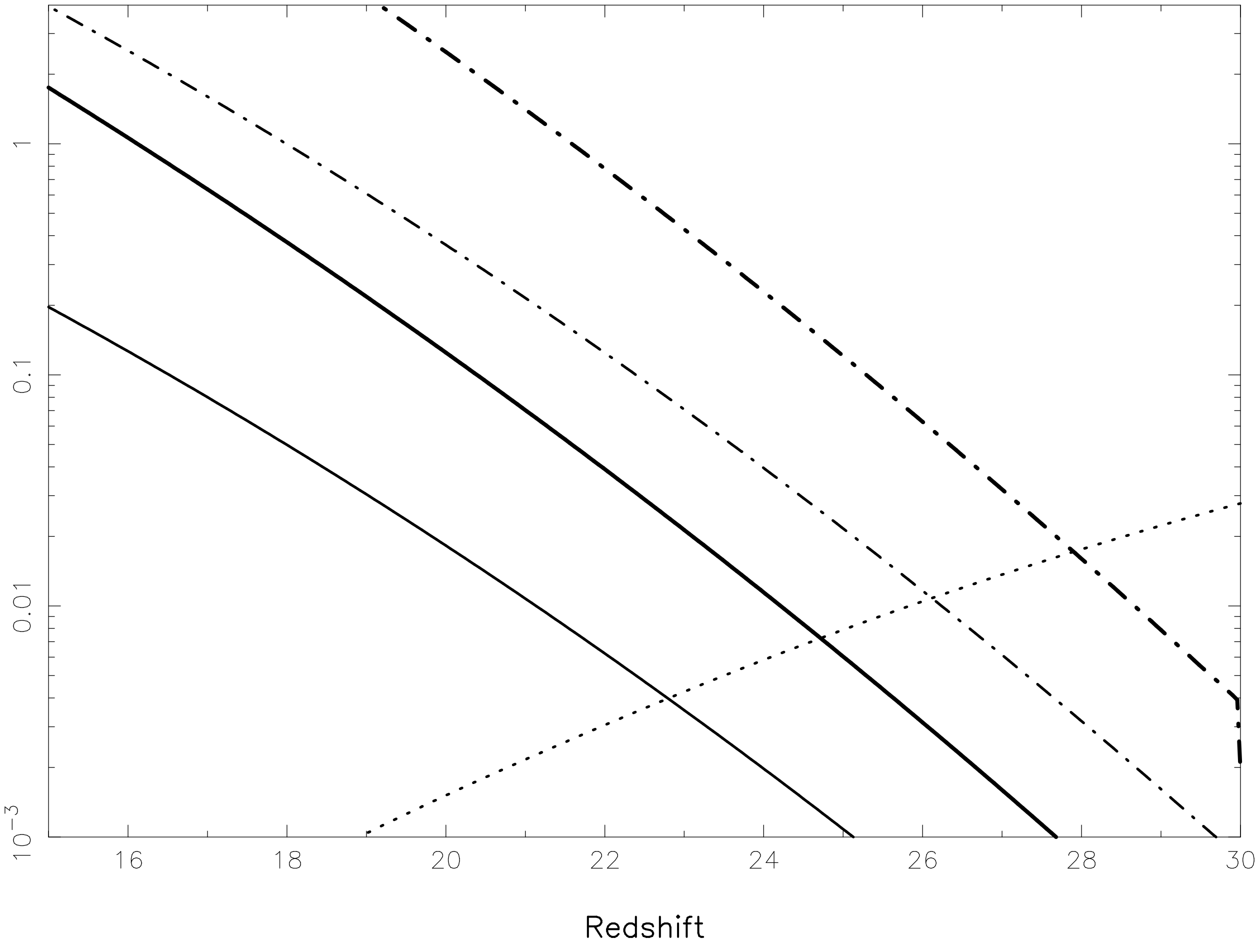

Figure 4. The figure shows the influence of Lyman-α photons as compared to particle collision and CMBR on the spin temperature (Eq. (2)) in regions that are not heated by x-ray radiation. Thin and thick solid lines correspond to $y_\alpha T_K/T_{\rm CMBR}$ and y_α for $\dot{N}_\gamma(0) = 10^{50}\,{\rm sec}^{-1}$ and the ratio of Lyman-α to ionizing flux $A = 2$, respectively. The thin and thick dot-dashed lines correspond to the same quantities for $A = 40$. The dotted line represents y_c.

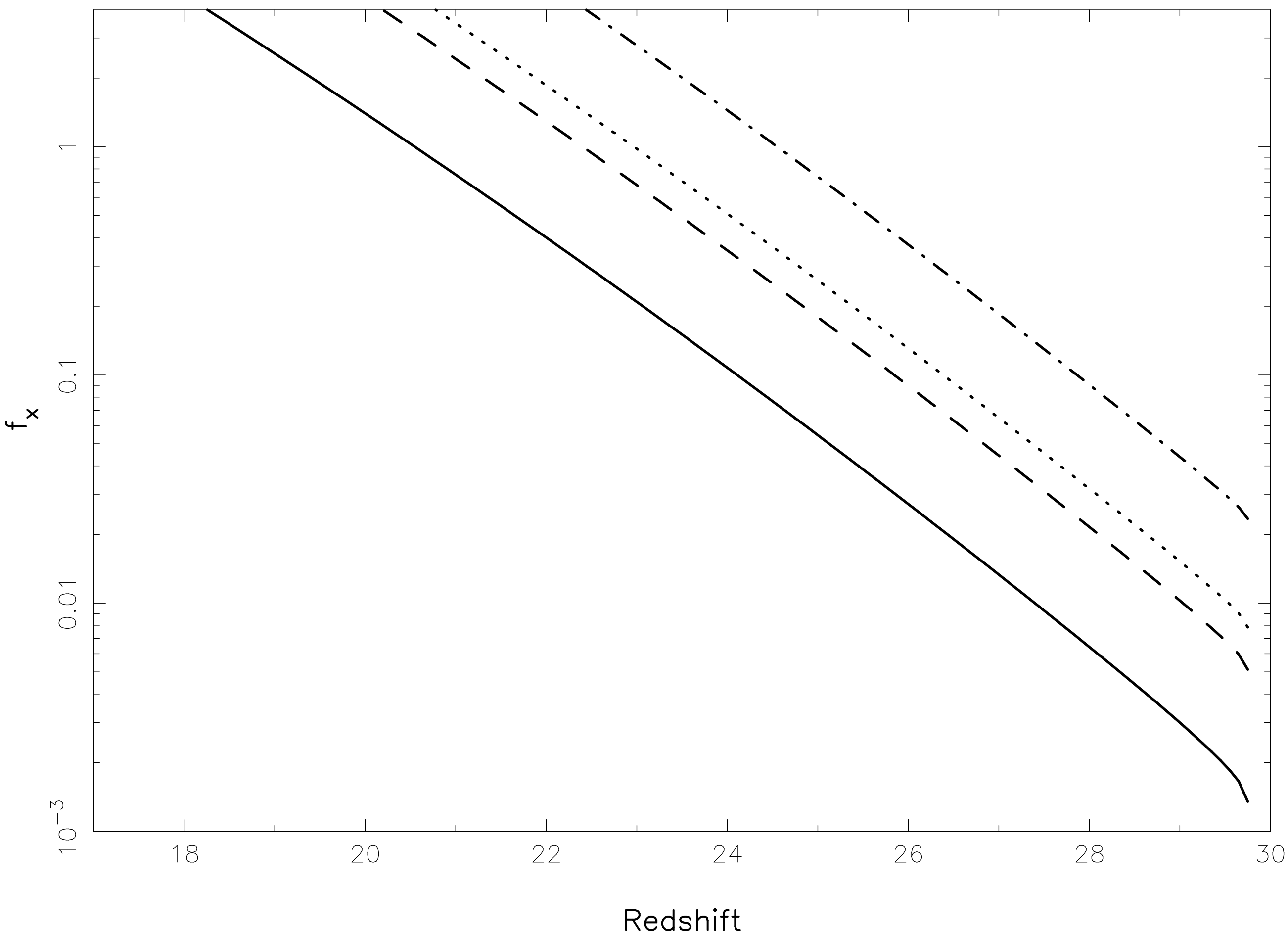

Figure 5. The evolution of the fraction of the universe heated by UV and soft xray, $f_{\rm x}$, is shown. All the models shown have $\dot{N}_\gamma(0) = 10^{50}\,{\rm sec}^{-1}$ and $C = 1$. Solid, dashed, and dot-dashed lines correspond to $q = 1$ and spectral indices $\alpha = \{1, 1.5, 2\}$, respectively. The dotted line corresponds to $q = 3$ and $\alpha = 1$

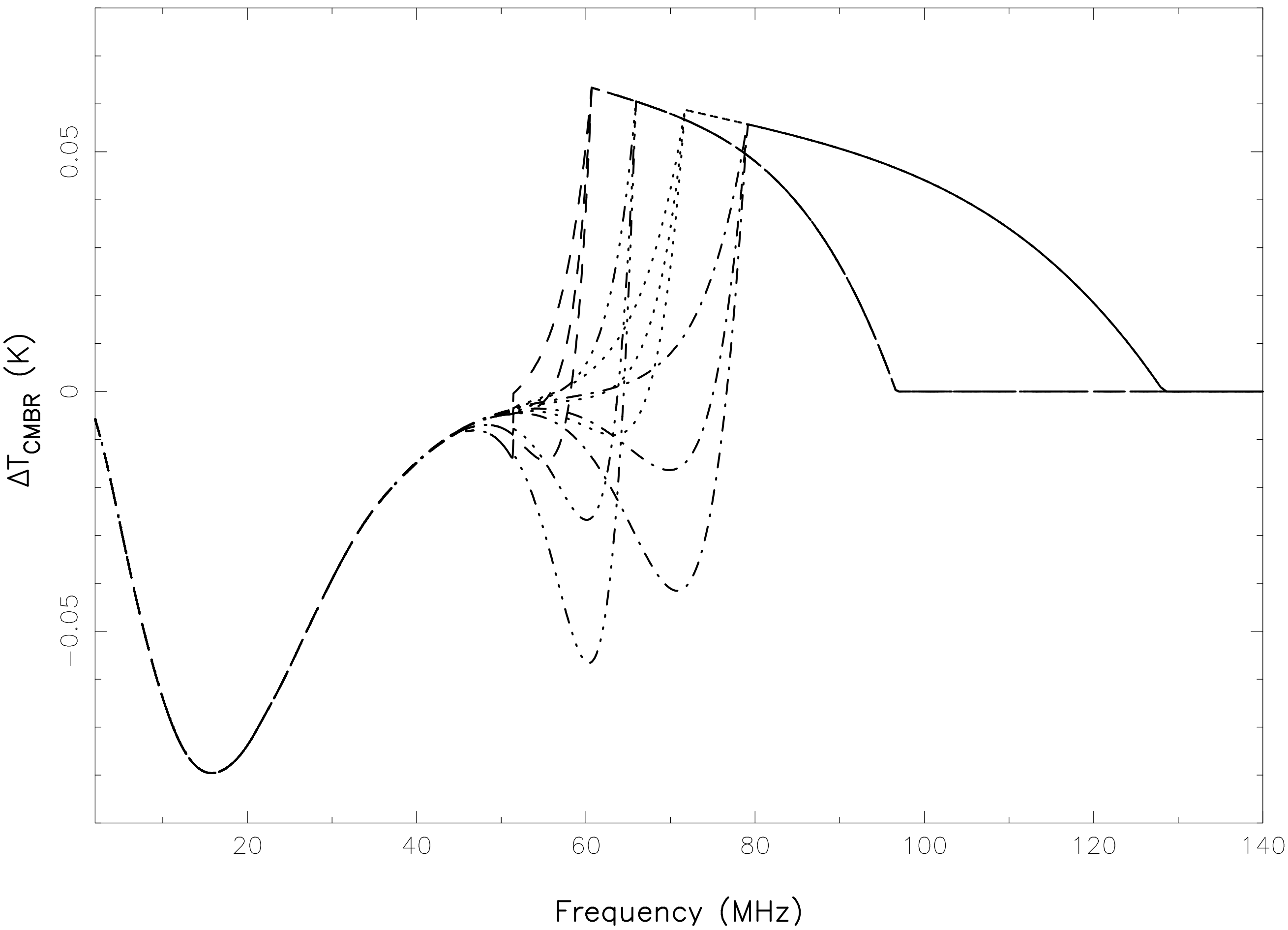

Figure 6. The HI signal from pre-reionization and reionization epochs is shown. The dashed and the dot-dot-dot-dashed curves correspond to an ionization history with $\dot{N}_\gamma(0) = 10^{50}\,\mathrm{sec}^{-1}$, $C = 1$. The dashed curves correspond to soft xray spectral index $\alpha = 1.5$ and, from top to bottom, to ratio of Lyman-α to ionizing flux ratios $\{2, 10, 20\}$. The dot-dot-dot-dashed curves correspond to $\alpha = 2$ with the same ratios of Lyman-α to ionizing flux. The dotted and dot-dashed curves correspond to an ionizing history with $\dot{N}_\gamma(0) = 10^{49}\,\mathrm{sec}^{-1}$, $C = 1$; the values of α and ratio of Lyman-α and ionizing flux have the same values as the curves for larger ionizing flux.

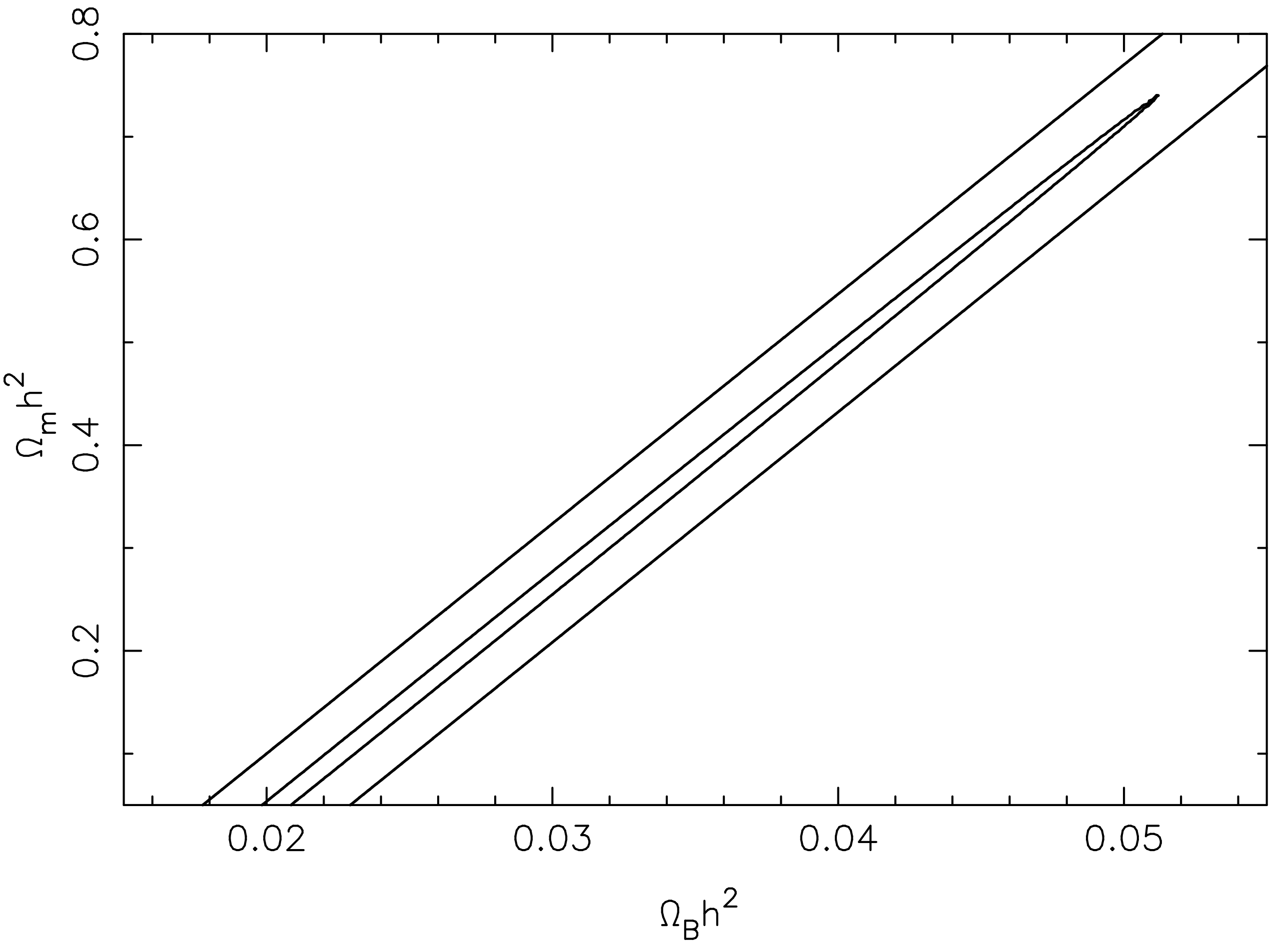

Figure 7. For pre-reionization signal, 2-σ contours in the plane of the cosmological parameters are shown. The inner and the outer contour correspond to $S_{\rm rms} = \{1, 3\}\,{\rm mK}$, respectively

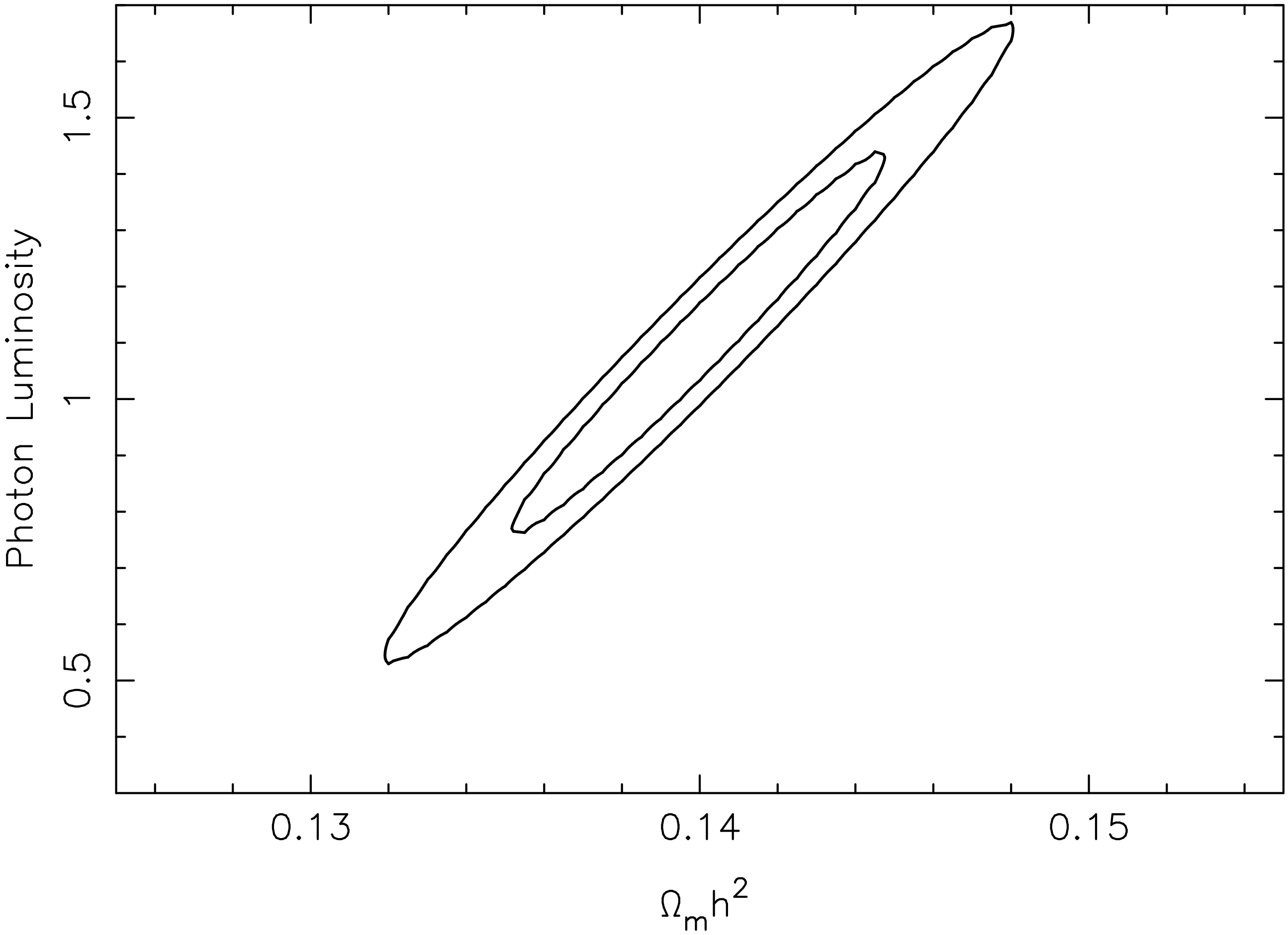

Figure 8. For the HI signal observed in emission, 1 and 2-σ contours in the plane of photon luminosity $\dot{N}_\gamma(0)/10^{49}$ and $\Omega_m h^2$ are shown (for details of the underlying model see text); the RMS noise is $S_{\rm rms} = 1\,{\rm mK}$.

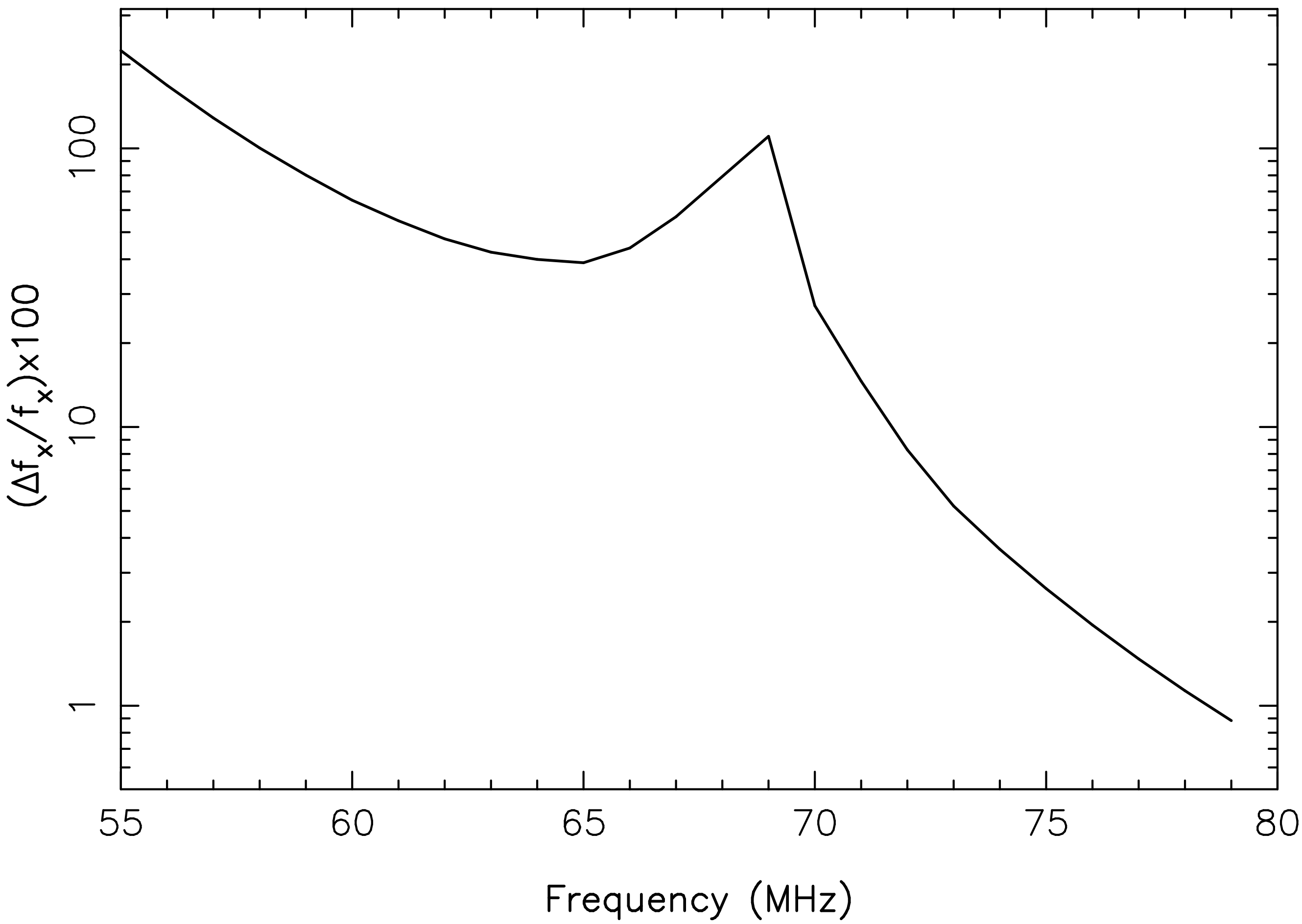

Figure 9. The percentage error on the fraction of universe heated by soft x-ray above CMBR temperature is plotted against the observing frequency. For details of the underlying model see text.